Science of Sintering, **38** (2006) 41-54

DOI: 10.2298/SOS0601041N

UDK 622.785:519.872

Computer Simulation of Free Settling and Skeletal Settling During Liquid Phase Sintering

Z. S. Nikolić

University of Nish, Faculty of Electronic Engineering
Department of Microelectronics, 18000 Nish, P.O. Box 73, Serbia

Abstract:

In recent years, a range of computer simulation models leading to a better understanding of liquid phase sintering phenomena, have been developed with the aim of simulating the detailed evolution of microstructure during grain growth. Some liquid phase sintered materials show both macrostructural and microstructural effects associated with gravity force. Therefore we will develop a numerical procedure for the estimation of how much gravity will influence domain (two-dimensional particle representation) growth, domain boundary migration and solid skeleton formation due to gravity induced segregation during liquid phase sintering. The method used for the simulation of a gravity field will be based on the settling procedure. Gravity induced settling will be separated into two stages -- Free Settling and Skeletal Settling. Isolated solid phase domains fall under gravity and slide down over the already settled domains (free settling). During settling they make point contacts with each other. Necks between them then form and start to grow until the equilibrium dihedral angle between the domain boundaries and the liquid is established. Thus a solid skeleton forms and skeletal settling of a connected solid structure takes place.

Keywords: *Liquid phase sintering, Free settling, Skeletal settling, Computer simulation.*

1. Introduction

The influence of gravitational effects on grain coarsening during liquid phase sintering (LPS) is of both fundamental and practical interest in materials science. It is well recognized that gravity contributes to separation of the solid and liquid phase [1]. Most investigations focus on the time dependent segregation based on combined temperature and gravitational fields for systems with a solid-liquid density difference. Because of that many experimental tests of diffusion phenomena, such as coarsening, are complicated by settling due to gravity since the time scales are relatively long compared to settling times. Even with higher contents of solid phase, there is progressive compact distortion with solid-liquid separation for long sintering times or at high sintering temperatures. This problem becomes more complicated by introducing coalescence that complicates grain coarsening especially at high solid volume fractions [2-7].

Many investigators have used a number of different numerical techniques to simulate grain coarsening. Recently the results of a computer simulation of boundary migration during

*) Corresponding author: znikolic@elfak.ni.ac.yu

LPS have been reported [8]. This approach was further applied for a computer study of LPS under gravity and microgravity conditions [9,10]. A similar method was developed by introducing basic, extended and combined models [11]. However, all these studies ignored the effects of pores on grain growth and on grain coarsening assuming zero porosity. In [12] a two-dimensional (2-D) method based on basic and mixed models for simulation of gravity induced microstructural evolution of porous structure during LPS was developed.

Gravity induced settling can be roughly separated into two stages; free settling of isolated particles and skeletal settling of a connected solid structure [13]. Free settling implies that isolated solid particles under gravity sink toward the sample bottom and slide down over the already settled particles. During settling they make point contacts with each other. At the same time between some of the contacting particles a neck will be formed. These necks start to grow until the equilibrium dihedral angle between the particle boundaries and the liquid is established. The formed solid skeleton (or skeletons) as a connected solid structure can also settle due to the gravity force. This process is skeletal settling (or compact slumping). A solid skeleton gives rigidity to the structure and the particles can settle with a restricted packing density. Even more, the solid skeleton can also densify through solid-skeleton densification.

Therefore, a particularly interesting approach would be the development of numerical models for simulation of free settling and skeletal settling, and their application to the estimation of how much gravity will influence grain growth, grain coarsening and solid-liquid separation during LPS. In this paper we will deal with a definition of a 2-D numerical method for simulation of microstructural evolution due to gravity during LPS. The method will be based on submodels for free settling and skeletal settling, as well as on domain topology instead of particle (grain) topology that means no shape restriction. In our approach the mentioned submodels can be applied as independent, or as sequential, but the two may overlap.

2. Domain topology

2.1. Domain definition

For particle representation in 2-D we will use an arbitrary domain, because circular shape particle (grain) representation is very simple and unrealistic. Even more, after a simulation time t ($t > 0$) most of the initially circular particles will no longer be circular due to the highly asymmetric diffusion field around and between them.

The domain as a closed boundary in 2-D (Fig. 1a) is fully defined by its boundary points - sites located on the domain boundary or on the phase interface, i.e.

$$D^{\ell} = \{ (x_k^{\ell}, y_k^{\ell}) \ (k = 1,2,...,n_{\ell}) \} \tag{1}$$

where n_{ℓ} is the number of its boundary points. If the rectangular experimental region is partitioned into subregions by a mesh defined by grid spacings Δx and Δy for two coordinates x and y respectively, then 2-D discrete domain representation will be as shown in Fig. 1b.

2.2. Domain translation

During LPS some domains can have a rigid body motion as a result of nonuniform concentration gradient over their boundaries. Even small changes in the domain location relative to one another can have a large effect on the resultant morphological model evolution. In this simulation an assumption will be made that the domains during movement will not overlap. It means that the domain movement must be restricted to those parts of the experimental region not already occupied by other domains, i.e.

$$D^{\ell}_{after} \bigcap_{j=1,2,...;\ \ell \neq j} D^{j} = \varnothing \ \text{ Then } \ D^{\ell} \mapsto D^{\ell}_{after}, \tag{2}$$

where D^{ℓ}_{after} is the domain position after its motion. If *a* and *b* are the translation distances in O*x* and O*y* directions, respectively, then the domain position after its translation will be defined as

$$D^{\ell} = \{ (x^{\ell}_k + a, y^{\ell}_k + b) \ \ (k = 1,2,...,n_{\ell}) \}$$

or

$$D^{\ell} = \{ (x^{\ell}_k + \Delta x, y^{\ell}_k + \Delta y) \ \ (k = 1,2,...,n_{\ell}) \} \tag{3}$$

on the mesh.

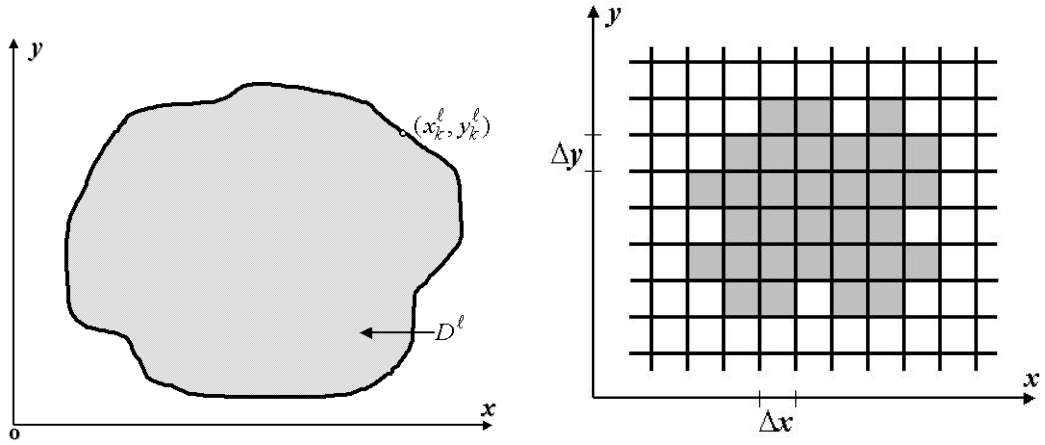

(a) (b)

Fig. 1. Schematic representation of 2-D domain defined (a) as a polygon (closed boundary), (b) by grid spacings Δ*x* and Δ*y*.

2.3. Domain coalescence

Domain coalescence will be simulated so that when two domains (Fig. 2a) come in contact with each other (Fig. 2b), they immediately coalesce (since their interfacial energy is reduced) to form a single domain (Fig. 2c). The algorithm for domain coalescence is explained below.

Let $D^{\ell 1}$ and $D^{\ell 2}$ be two domains in contact with each other. If the condition

$$D^{\ell 1} \cap D^{\ell 2} \geq m, \tag{4}$$

where *m* is the minimal number of neighboring boundary points of these domains related by the pair of indexes (i, j) and $(i+1, j)$ or (i, j) and $(i, j+1)$, is fulfilled then the domains $D^{\ell 1}$ and $D^{\ell 2}$ will be replaced by a new domain (Fig. 2c)

$$D^{\ell 1} = D^{\ell 1} \cup D^{\ell 2}. \tag{5}$$

3. Model topology

Let there be a mixture of two powders: a major component that forms the particulate solid, and an additive phase as a liquid-producing component. It will be assumed that the liquid perfectly wets and spreads to cover the solid particle surfaces, so that a liquid layer will separate them.

A time-dependent microstructure will be represented digitally by discretizing the microstructure on 2-D square lattice (simulation lattice). All information connected to the lattice will be stored in the integer matrix $\| e_{ij} \|_{n\times m}$, where the value of the element e_{ij} indicates the phase present at the point (occupying the lattice sites) (i, j), so that

$$e_{ij} = \begin{cases} < 0 & \text{pore phase, i.e. } -1,-2,...,-P \\ 0 & \text{liquid phase} \\ > 0 & \text{solid phase, i.e. } 1,2,...,S \end{cases} \quad (6)$$

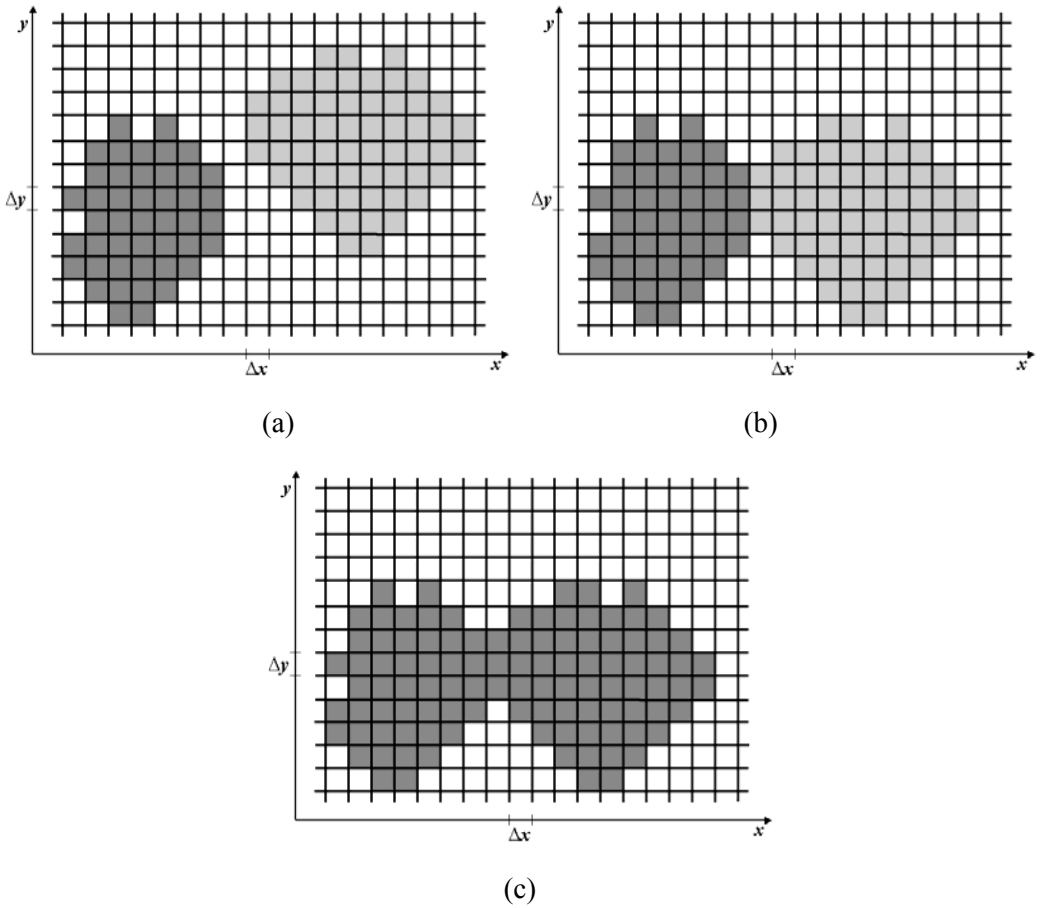

Fig. 2. Schematic representation of coalescence of two domains. (a) Separated domains. (b) Contacting domains. (c) Coalesced domains.

The digitized microstructure consists of *S* solid-phase domains and *P* pore-phase domains, both phases in liquid matrix. A model system of $S + P$ domains will be located within the smallest enclosing square box. Both *S* and *P* domains will be represented as arrays of boundary points (Eq. (1)), i.e.

$$D^s = \{(x_k^s, y_k^s)\ (k = 1,2,...,n_s)\} \quad (s = 1,2,...,S) \quad (7)$$

$$D^p = \{(x_k^p, y_k^p)\ (p = 1,2,...,n_p)\} \quad (p = 1,2,...,P) \quad (8)$$

where n_s and n_p are the number of the boundary points for the *s*-th solid- and *p*-th pore-domain, respectively. Here the solid-phase and pore-phase domains are defined by contiguous

points (lattice sites) labeled with the same number according to the definition (6), that is, the contiguous points labeled with the same positive number form a solid-phase domain and the contiguous points labeled with the same negative number form a pore-phase domain. A domain (grain) boundary exists between neighboring domains labeled with different integer numbers (solid-solid interface) or between domain and liquid phase (solid-liquid interface).

We will assume that the liquid penetrates domain boundaries of the solid phase. Therefore, domains of the solid phase are entirely surrounded by liquid, a thin film of which is always present between neighboring solid-phase domains. Since the liquid wets the solid phase perfectly pore domains are therefore separated from the solid/liquid boundary by at least a thin film of liquid.

During sintering pore- and solid-phase domains co-evolve: pore domains shrink, solid-phase domains (grains) grow or shrink.

3.1. Pore phase

The pores are holes caused by trapped gases. On Earth these pores are driven out of the sample during sintering by buoyancy, i.e. by the tendency to move upward. In our model the pores will be treated as isolated and mobile.

We will consider pore domains to behave not identically to solid-phase domains and they are characterized by pore migration, which will be modeled by Brownian motion [12] (random translation) defined by modified translation (3) as follows

$$D^{\ell} = \{ (x_k^{\ell} \pm \Delta x, y_k^{\ell} \pm \Delta y) \ \ (k = 1,2,...,n_{\ell}) \}, \tag{9}$$

so that each pore will be chosen at random and translated in random X or Y or X-Y direction (in 8-near points directions, so called 8-directional model [14]) if and only if the modified condition (2)

$$D_{after}^{\ell} \bigcap D^{j} = \varnothing \quad \text{Then} \quad D^{\ell} \mapsto D_{after}^{\ell} \tag{10}$$
$$j=1,2,...,S;\ j=-1,-2,...,-P;\ \ell \neq j$$

is fulfilled. In that case each pore will attempt one change during one time increment Δt. For a selected pore domain the simulator (see Section 3.3) checks in each iteration (time step) condition (10) and makes a random translation of the pore (9).

The pore growth occurs by coalescence, which will be simulated applying the domain coalescence method defined by Eqs. (4) and (5). When two pores come in contact with each other by random walk, they immediately coalesce to form a single pore. After coalescence two pore domains D^{p1} and D^{p2} will be replaced by a new pore domain

$$D^{p1} = D^{p1} \cup D^{p2}$$

and corresponding domain elements $\{e_{ij}\}$ of the integer matrix will be replaced by relation (a single pore will be labeled with a smaller integer number of the previous two)

$$e_{ij}\{e_{ij} = -p2 \,|\, (i,j) \in D^{p2}\} \mapsto e_{ij}\{e_{ij} = -p1 \,|\, (i,j) \in D^{p2}\}.$$

The pore filling process will be considered in a way similar to Park *et al.* [15] who developed models for liquid flow into isolated pores. It was assumed that the initially spherical pores exist within a solid-liquid system in which the grain shape is in equilibrium with the liquid menisci. In the initial stage the pores are stable and individual liquid menisci are maintained between grains around the pores. During sintering when the grain growth reaches a critical point meniscus radius becomes equal to the radius of pore. As the grains grow beyond the critical point pores start to decrease. The balance of the liquid pressure between menisci at the pore and those at the surface is now broken and liquid can flow rapidly into the pore. Our model assumes that for each pore there is a critical grain size required for filling. This model was already applied for computer simulation of grain

coarsening during LPS [16].

3.2. Solid skeleton

During LPS solid-phase domains will settle due to gravity. As the domains arrive over the already settled domains they make point contacts with each other and necks between them form. Neck growth will end when the equilibrium dihedral angle between the domain boundaries and the liquid is established. Thus a solid skeleton forms.

If there is a set of *K* solid-phase domains in which each domain have contact with one or several other solid-phase domains of type (7), then the solid skeleton (SS) will be defined as an union of these contacting domains, i.e.

$$SS = \bigcup_{k=1}^{K} D^{h(k)}$$

where $h(k)$ is the vector of ordinal number of domains that form the skeleton. The contact between two adjacent *i*-th and *j*-th solid-phase domains will be defined by the set of data

$$\{i, j, CP_{ij}, D_{ij}\} \quad (i \neq j),$$

where CP_{ij} is the number of common boundary points (contact points or points that form the neck), and D_{ij} is the bridging link length defined by the relation

$$D_{ij} = \sqrt{(x_c^i - x_c^j)^2 + (y_c^i - y_c^j)^2},$$

where (x_c^s, y_c^s) and (x_c^q, y_c^q) are the center position of contacting domains.

The skeleton network is made up of a unique, interconnected set of connected solid-phase domains. Each domain in the network has to have a set of data with information about the nearest neighbors

$$\{k, n_k; m_1, m_2, ..., m_{n_k}\} \quad (k = 1,2,...,K),$$

where n_k and $m_1, m_2, ..., m_{n_k}$ are the number of neighboring solid-phase domains and their ordinal numbers.

The skeleton network, given as a system of functions of some topological parameters, changes monotonically with time by adding new solid-phase domains. If

$$\{D_{ij}^k(t)\} \quad (i \neq j)$$

is the *k*-th skeleton network link length at time t, then a new network state will be determined by increasing its length by adding new domains during skeleton settling.

3.3. Simulator

For the computation of liquid phase concentration (the numerical solution of the diffusion equation) and simulation of all solution-reprecipitation effects the finite-difference technique will be used [8].

The main topology of the model system given by (7) and (8) is time dependent, i.e.

$$D^s = D^s(t) \quad (s = 1,2,...,S) \tag{11}$$

$$D^p = D^p(t) \quad (p = 1,2,...,P) \tag{12}$$

During the simulation process the simulator continuously checks for possible new solid- and pore-domain positions, where the domains (11) and (12), as a function of time, will be updated by

$$D^s(t+\Delta t) = D^s(t) + \Delta D^s(\Delta t) \quad (s = 1,2,...,S)$$

$$D^p(t+\Delta t) = D^p(t) + \Delta D^p(\Delta t) \quad (p = 1,2,...,P)$$

where new subdomains (domains' increments) $\Delta D^s(\Delta t)$ will be the result of current dissolution and precipitation processes, and $\Delta D^p(\Delta t)$ the result of pore growth and pore filling processes. All updated topological information will be recorded and saved for each time interval for the next analysis and computation.

4. Settling

4.1. Stokes' law

Systems with a large density difference between the liquid and solid ($\rho_s - \rho_L$) are characterized by macro- and micro-structural effects associated with gravity. This is a particular problem for tungsten heavy alloys.

Under Earth-based experimental conditions Stokes's law settling usually dominates microstructure formation [5]. The settling time for solid domains to travel the average separation distance $\langle\lambda\rangle$ between domains [11] in a liquid matrix can be calculated as

$$\tau_{settl} = \frac{\langle\lambda\rangle}{v_{settl}} \quad (v_{settl} = \frac{2g\langle r\rangle^2(\rho_s - \rho_L)}{9\eta}), \tag{13}$$

where g is the gravitational acceleration, $\langle r\rangle$ is the average domain radius and η is the liquid viscosity.

4.2. Settling procedure

The settling procedure will be applied to simulate the gravity force. The solid-phase domains will be subjected to a simulated gravity field [8]: they fall under gravity and slide down over the already settled solid-phase domains. Such a procedure will be applied to each solid-phase domain starting with this one having the lowest position in the vertical direction of experimental region. This procedure will be modeled by domain translation (3) along the gravitational direction, i.e.

For $i = 1$ To S
$D^i = \{(x_k^i, y_k^i) \ (k = 1,2,...,n_i)\}$
$D_{after}^i = \{(x_k^i, y_k^i - \Delta y) \ (k = 1,2,...,n_i)\}$
If $D_{after}^i \bigcap_{j=1,2,...,S;\ j=-1,-2,...,-P;\ i\neq j} D^j = \varnothing$ Then $D^i \mapsto D_{after}^i$
Next i

(14)

Packing of solid-phase domains will be the result of translation in the gravity direction or combined translation in the horizontal (sliding over settled domains) and in the vertical (gravity) direction. In that sense, the previous algorithm (14) must be generalized as follows

$$\begin{array}{l}\text{For } i=1 \text{ To } S\\ \quad D^i=\{(x_k^i, y_k^i)\ \ (k=1,2,...,n_i)\}\\ \quad D_{after}^i=\{(x_k^i \pm \Delta x, y_k^i-\Delta y)\ \ (k=1,2,...,n_i)\}\\ \quad \text{If} \quad D_{after}^i \bigcap_{j=1,2,...,S;\ j=-1,-2,...,-P;\ i\neq j} D^j=\varnothing \quad \text{Then } D^i \mapsto D_{after}^i\\ \text{Next } i\end{array} \tag{15}$$

where the sign $\dot{+}$ means that the signs + and - will be taken at random or both ones in sequence. Therefore densification results from the uniform center-to-center motion of neighboring domains. Horizontal and vertical translations combined in a sequence or in parallel give way to reaching a local equilibrium system state.

5. Results and discussions

For simulation of LPS under gravity conditions we will use two submodels for Free Settling and Skeletal Settling. These models will be tested in order to conduct a study of diffusional and gravitational effects on microstructural development of W-Ni system. The following data will be used: the equilibrium concentration of liquid in contact with the solid: 35 at.% W [17]; the diffusion coefficient in the liquid W-Ni alloy 10^{-9} m^2s^{-1} [18]; the sintering temperature: 1750 K; liquid viscosity: $5\cdot10^{-3}$ Pas (for liquid nickel); the acceleration: 9.81 ms^{-2}; the liquid-solid density difference: 9 gcm^{-3}, and the interfacial energy 0.8 Jm^{-2}.

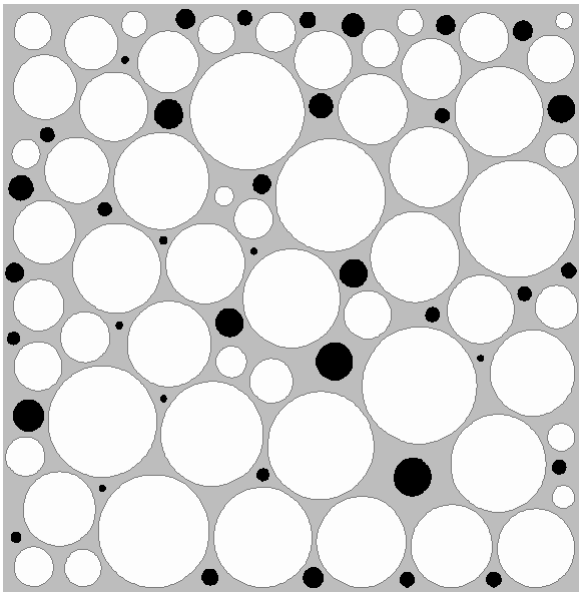

Fig. 3. Initial model of porous structure (white colored regions are solid phase, black colored regions are pores, and gray colored region is liquid phase).

The porous structure will be represented by *N* domains: *S* domains as the solid phase and *P* domains as the pore phase, so that $S+P=N$. An initial model of $N=S+P=58+38$ domains (Fig. 3) was obtained by applying random generating method described in detail elsewhere [8] and assuming the radius range $10-60\ \mu m$ with the initial average domain radius of $34\ \mu m$ for solid W, and the pore radius range $5-25\ \mu m$ with the

initial average pore radius of $9.7\,\mu m$. Pore coalescence and solid-phase coalescence parameters (*m* in Eq. (4)) were 2 and 5, respectively. The grid mesh was 300◈300.

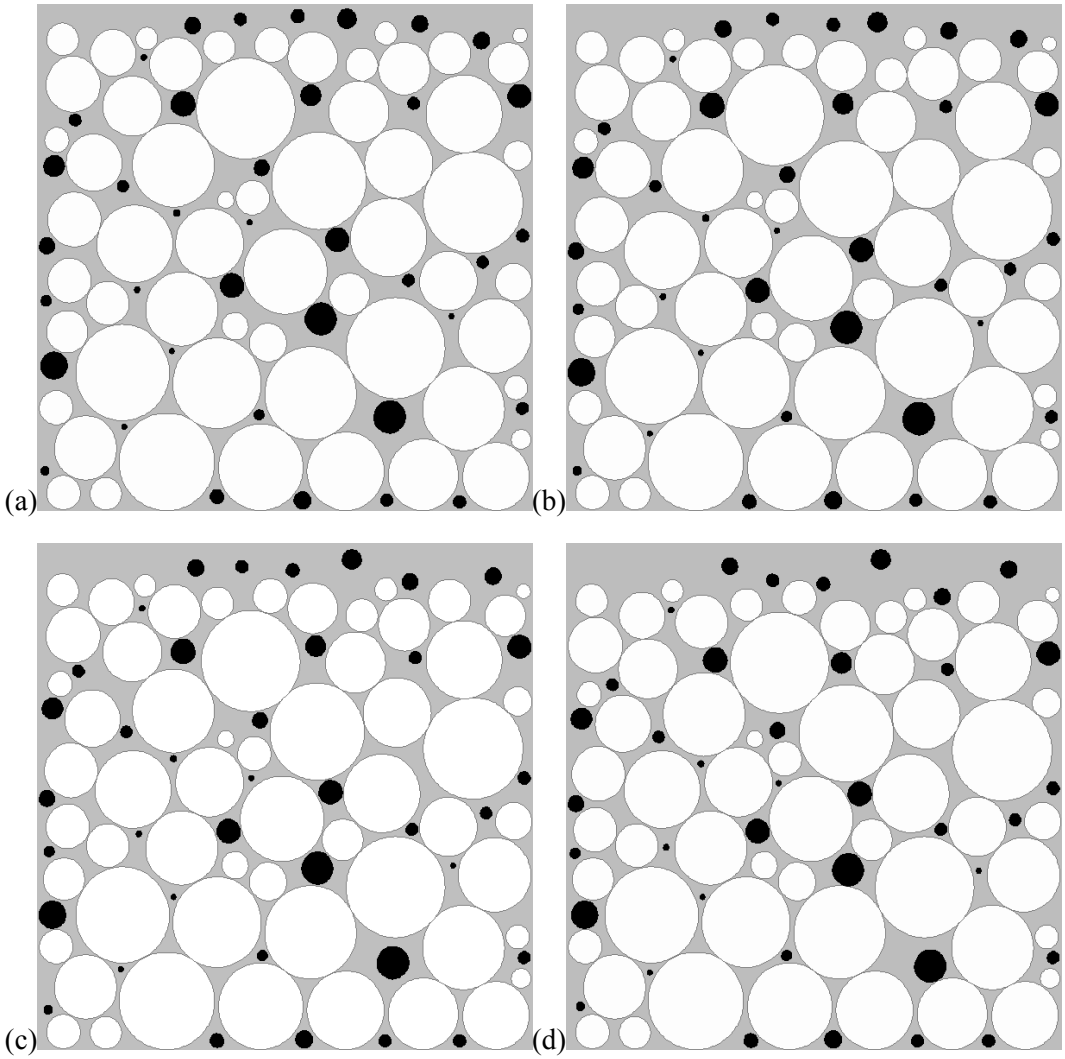

Fig. 4. Four typical snapshots of the computed microstructure (white colored regions are the solid phase, black colored regions are pores, and the gray colored region is the liquid phase) evolving under different sintering time (a) 0.1, (b) 0.2, (c) 0.3 and (d) 0.5 min.

The solution-precipitation process and coarsening process were modeled as it was described in detail elsewhere [8]. Our simulation method will be based on two submodels for solution-precipitation and coarsening, as well as on gravitational settling (algorithm (14) or (15)). LPS starts with the solution-precipitation process characterized by dissolution of smaller solid domains at the solid/liquid interface, dissolved atoms diffuse through the liquid, and preferentially precipitate onto larger domains. Since under Earth-based experimental conditions Stokes's law settling usually dominates microstructure formation, the settling time for solid-phase domains to travel the average separation distance in the liquid matrix will be calculated by applying this law. At settling time (13) the gravity force effect will be simulated by the settling procedure in which the solid-phase domains are subjected to a simulated gravity field (Free Settling): they fall under gravity and slide down over the already settled domains. This domain displacement will be modeled by domain translation along the gravitational direction (algorithm (15)), where the domain position after its translation will be

restricted to those parts of the experimental region not already occupied by other domains. As the domains arrive over the already settled domains they can make point contacts with some of them or with each other. It will depend on the current topology of model constituents solid-phase domains - pore domains - liquid phase.

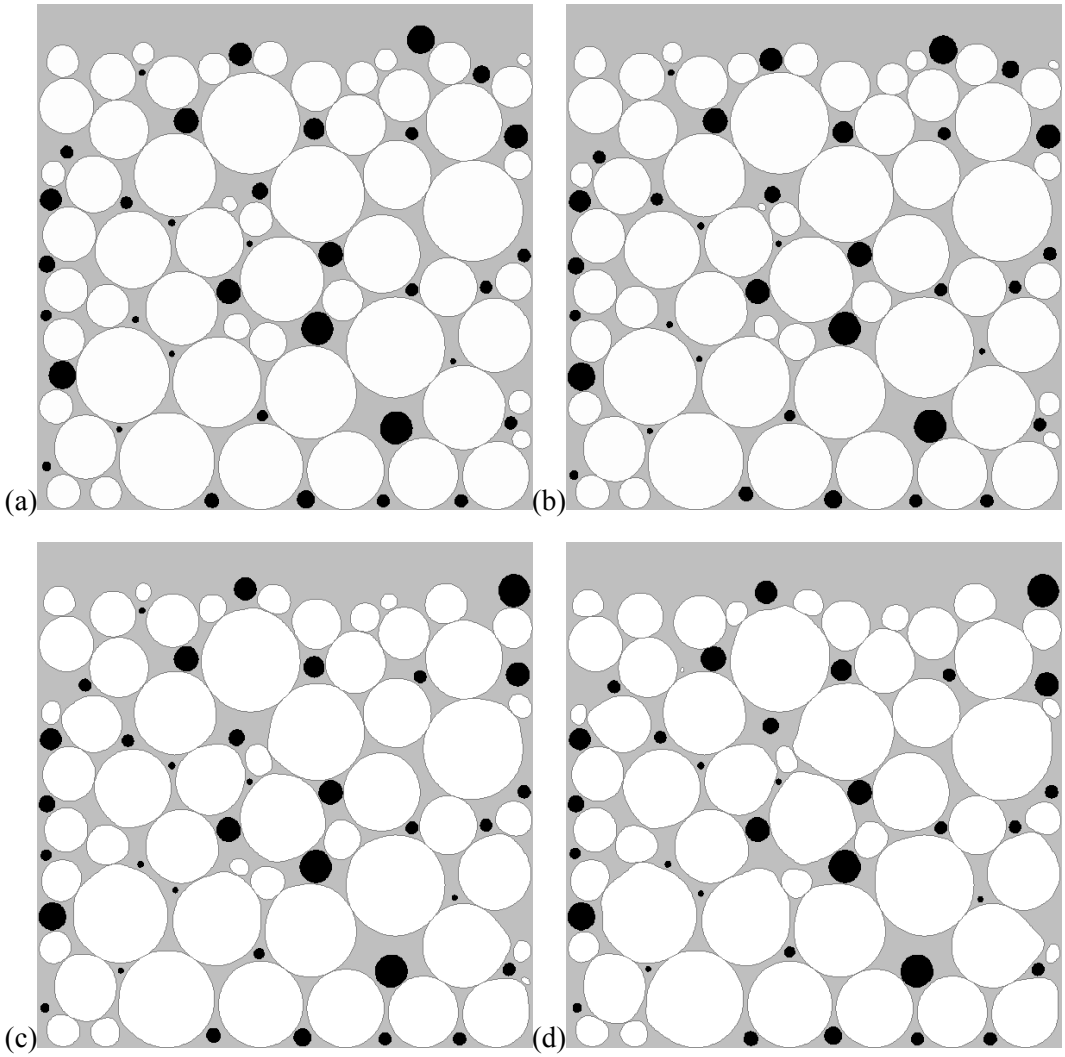

Fig. 5. Four typical snapshots of the computed microstructure (white colored regions are the solid phase, black colored regions are pores, and the gray colored region is the liquid phase) evolving under different sintering time (a) 10, (b) 20, (c) 40 and (d) 60 min.

Figures 4 and 5 show microstructural evolution obtained by the Free Settling model. Shown on Fig. 4 are computed microstructures to illustrate step by step (short time interval of 0.1 s) the gravity induced microstructural changes during LPS of W-Ni. After a very short time, solution-diffusion-precipitation processes are just beginning to occur along the (solid-phase) domain/liquid boundary interfaces. Under Earth-based experimental conditions, Stokes' law settling usually dominates microstructure formation. The smaller dissolving domains give way to slow settling and densification by packing of small and large domains. The simulated results show almost complete settling in a very short sintering time, i.e. in a few minutes after liquid formation. This result is very similar to the results of German [19]. In his investigation of solid settling during LPS of tungsten-nickel-iron alloys the calculated maximum settling time using Stokes' law with a varying grain size and the same value for

liquid viscosity as in our simulation gave complete settling in 4 to 6 minutes. Note that Eliasson [20] reported more rapid settling during LPS of the dilute tungsten heavy alloy compositions because of agglomeration. The total settling time was less than 1 minute. However, simulation with a higher viscosity of $18 \cdot 10^{-3}$ Pas leads to times of 14 to 22 minutes for complete settling [19].

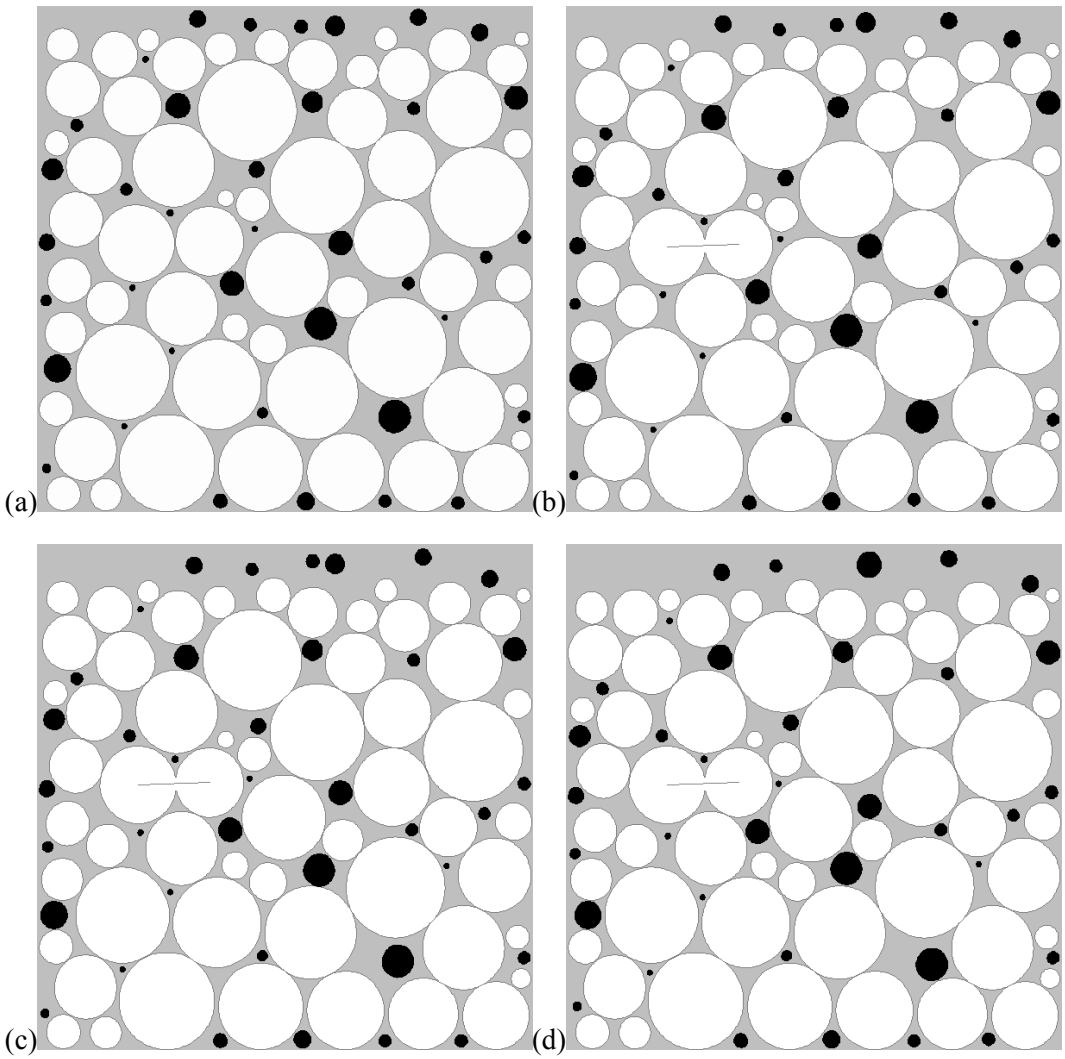

Fig. 6. Four typical snapshots of the computed microstructure (white colored regions are the solid phase, black colored regions are pores, and the gray colored region is the liquid phase; the gray straight line represents the skeletal network) evolving under different sintering time (a) 0.1, (b) 0.2, (c) 0.3 and (d) 0.5 min.

For longer sintering time (Fig. 5) shape distortion of the solid-phase domains can be observed. Pure tungsten dissolved into the liquid and diffused through the liquid matrix precipitates as a W(Ni) solid solution on the larger domains. The largest shape distortion in the center-to-center direction is a result of interdomain (interparticle) diffusion interactions at relatively small interparticle distances. The smaller domains tend to be preferentially located near the large domains, as suggested in Ref. [21], because the large domains always grow, resulting in the surrounding domains being small. After 60 min some of the smaller domains have disappeared (Fig. 5d). After a very long time most of the smallest domains will have disappeared, some of them will be still dissolving and the bigger domains will be growing

only. It can be seen that the domains principally assume a rounded shape because the amount of liquid is fairly large. Even more, in a late stage of LPS, it can be expected that some of the domain contacts can be approximately flattened. Because the present simulation is performed without the shape restriction, no overlapping contours were found.

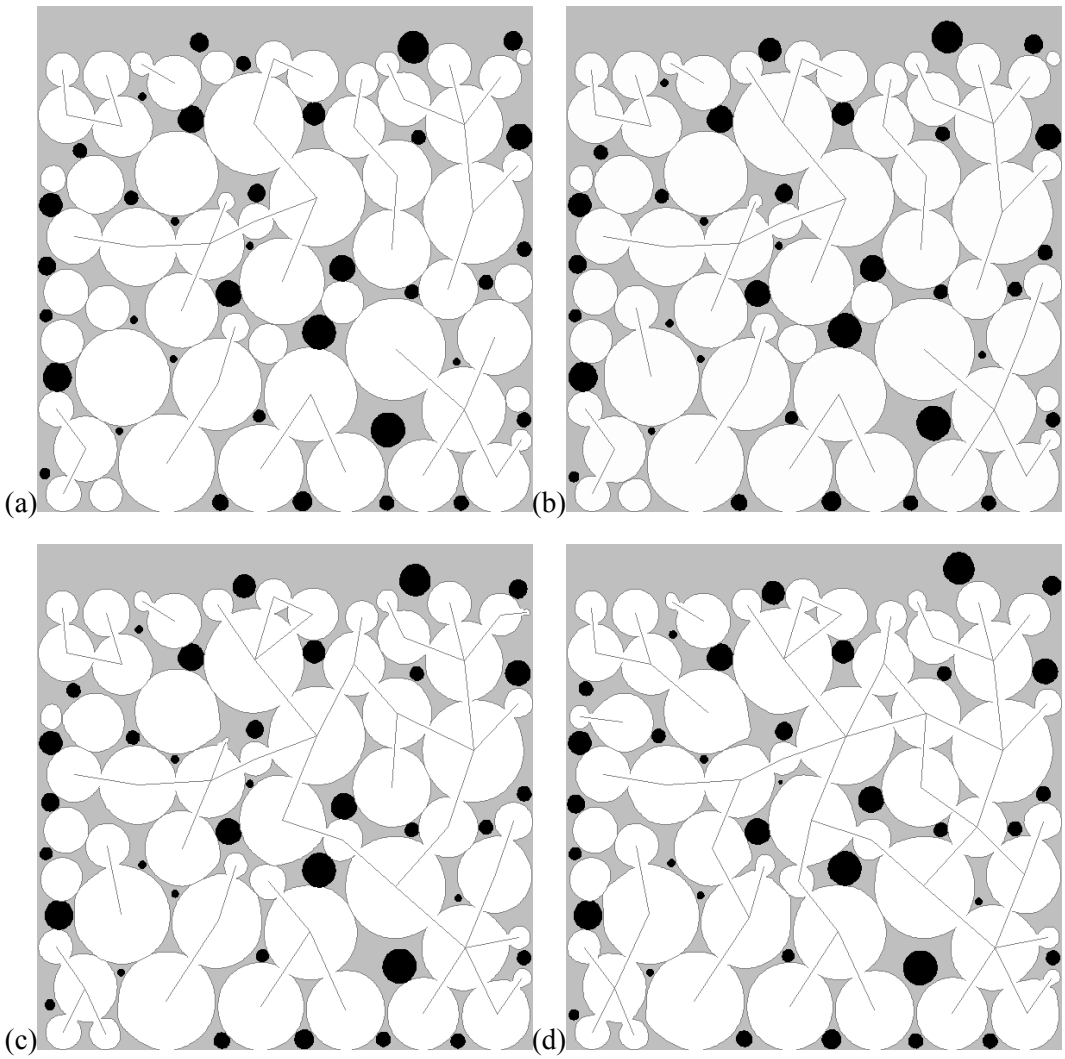

Fig. 7. Four typical snapshots of the computed microstructure (white colored regions are the solid phase, black colored regions are pores, and the gray colored region is the liquid phase; the connected gray straight line segments represent skeletal networks.) evolving under different sintering time (a) 10, (b) 20, (c) 40 and (d) 60 min.

The skeletal settling model also assumes that as the solid-phase domains arrive over the already settled domains they make point contacts with each other. However, now necks between them form and start to grow until the equilibrium dihedral angle between the domain boundaries and the liquid is established. Thus a solid skeleton forms. It means that this model simulates complex settling consisting of "free settling" for isolated domains and "skeleton settling" for connected domains.

At an early sintering time the computed liquid phase sintered microstructures are very similar to the previous one, i.e. no big differences exist between them. It can be seen that during rapid free settling (short sintering times, Fig. 6) only one skeleton (solid straight line) will be formed. However, for longer sintering time a systematic increase in the number of

necks (contacts) along the gravity direction can be seen for each next settling time as a consequence of solution-precipitation between two successive settling times. It also means that the number of skeletons increases or decreases (9, 10, 7 and 5 in Figs. 7a, 7b, 7c and 7d respectively) and their lengths usually increase during LPS. The decrease of the number of skeletons in time is a result of coalescence of two or more solid skeletons. It can be seen that microstructures obtained by this model differ from previous ones obtained by the free settling submodel. Shape distortion still exists but the tungsten skeletal structure tends to inhibit solid-liquid separation.

Note that skeletal settling occurs in systems characterized by a denser solid phase. The microstructure after the early stage of free settling is just such a dense solid phase.

6. Conclusion

A 2-D numerical method for simulation of microstructural evolution during LPS under gravity condition has been described. Domain topology was used instead of the usually used particle (grain) topology because it introduces no shape restriction. The porous structure was represented by N domains: S domains as the solid phase and P domains as the pore phase, so that $S + P = N$. We considered pore domains to behave not identically to solid-phase domains and to be characterized by pore migration (which was modeled by Brownian motion), pore coalescence and pore filling. The simulation method was based on two numerical submodels for the simulation of free settling and skeletal settling of solid-phase domains, where both submodels can be applied as independent, or as sequential, but they may also overlap. These models were tested in order to conduct a study of diffusional and gravitational effects on microstructural development during sintering of the W-Ni system. The simulated results showed almost complete settling (with separation of the solid and liquid phase) in a very short sintering time, i.e. in a few minutes after liquid formation. For longer sintering time shape distortion of solid-phase domains were observed, whereas the largest shape distortion was in the center-to-center direction as a result of interdomain diffusion interactions at relatively small interdomain distances. It was shown that microstructures obtained by the skeletal settling submodel differ from microstructures obtained by the free settling submodel -- shape distortion was also observed but the tungsten skeletal structure tended to inhibit solid-liquid separation.

Acknowledgments

The present work was performed under the project (No 1832) *Synthesis of Functional Materials According to the Tetrade "Synthesis-Structure-Properties-Application"* supported financially by the Ministry of Science and Environmental Protection of the Republic of Serbia.

References

1. R. M. German, Yixiong Liu and A. Griffo, Metal. Materials Trans. A, 28A (1997) 215.
2. W. J. Huppmann, H. Riegger, 13 (1977) 243-247,
3. D. N. Yoon, W. J. Huppmann, Acta Metall., 27 (1979) 973-977.
4. T. H. Courtney, Metall. Trans. A, 8A (1977) 671-677.
5. T. H. Courtney, Metall. Trans. A, 8A (1977) 679-684.

6. T. H. Courtney, Metall. Trans. A, 8A (1977) 685-689.
7. R. M. German, A. Bose, and S.S. Mani, Metull. Trans. A, 23 (1992) 211.
8. Z. S. Nikolic, Journal of Materials Science, 34(1999) 783-794.
9. Z. S. Nikolic, Science of Sintering, 31 (1999) 83-89.
10. Z. S. Nikolic, Science of Sintering, 32, Special Issue (2000) 61-69.
11. Z. S. Nikolic, Science of Sintering, 34 (2002).
12. Z. S. Nikolic, VI Scientific Meeting Physics and Technology of Materials FITEM'05, Čačak, 2005, pp. 39-40.
13. T. M. Courtney, Scripta Materialia, 35 (1996) 567-571.
14. R. C. Gonzales and R.E. Woods, Digital Image Processing, Prentice Hall, 2002.
15. Hyo-Hoon Park, Seong-Jai Cho and Duk N. Yoon: Met. Trans. A, 15A (1984) 1075.
16. Z. S. Nikolic, Materials Science Forum, Vol. 494 (2005) 387-392.
17. M. Hansen and K. Anderko, Constitution of Binary Alloys, McGraw-Hill, New York, 1958.
18. Y. Ono and T-Shigematsu, J. Japan Inst. Met., 41 (1977) 62.
19. R. M. German, Metall. Mater. Trans., 26A (1995) 279.
    Eliasson, Ph.D. Thesis, The Royal Institute of Technology, Stockholm, Sweden, 1992.
20. M. Marder, Phys. Rev. Lett. 55 (1985) 2953.

Садржај: *Низ симулационих модела, који омогућују боље разумевање феномена синтеровања у присуству течне фазе, развијен је последњих година са циљем симулације детаља еволуције микроструктура током раста зрна. Неки материјали синтеровани у присуству течне фазе показују микроструктурне и микроструктурне ефекте повезане са силом гравитације. Ми ћемо зато развити нумерички метод за оцену утицаја раста домена (дво-димензионална репрезентација честице), померање границе домена и формирање скелетона чврсте фазе због таложења изазаваног гравитацијом током синтеровања у присуству течне фазе. За симулацију гравитационог поља биће коришћена тзв. settling процедура. Таложење услед гравитације одвијаће се у два стадијума: слободно таложење и таложење скелетона. Изоловани домени чврсте фазе падају под утицајем гравитације преко већ раније наталожених домена (слободно таложење). Током таложења они формирају једно-тачкасте контакте један са другим. Након тога долази до формирања вратова и њиховог раста до достизања равнотежног угла између границе домена и течне фазе. Истовремено са тим формирају се скелетони чврсте фазе па таложење скелетона може да започне.*

Кључне речи: *Синтеровање у присуству течне фазе, слободно таложење, таложење скелетона, компјутерска симулација.*